

# Propagation model for estimating VOR bearing errors in the presence of windturbines - hybridation of parabolic equation with physical optics

Christophe Morlaas, Alexandre Chabory, Bernard Souny

## ► To cite this version:

Christophe Morlaas, Alexandre Chabory, Bernard Souny. Propagation model for estimating VOR bearing errors in the presence of windturbines - hybridation of parabolic equation with physical optics. EuCAP10, 4th European Conference on Antennas and Propagation, Apr 2010, Barcelona, Spain. pp 1-5, 2010. <hal-01022224>

HAL Id: hal-01022224

<https://hal-enac.archives-ouvertes.fr/hal-01022224>

Submitted on 23 Sep 2014

**HAL** is a multi-disciplinary open access archive for the deposit and dissemination of scientific research documents, whether they are published or not. The documents may come from teaching and research institutions in France or abroad, or from public or private research centers.

L'archive ouverte pluridisciplinaire **HAL**, est destinée au dépôt et à la diffusion de documents scientifiques de niveau recherche, publiés ou non, émanant des établissements d'enseignement et de recherche français ou étrangers, des laboratoires publics ou privés.

# Propagation model for estimating vor bearing error in the presence of windturbines – hybridation of parabolic equation with physical optics

C. Morlaas\*, A. Chabory\*, B. Souny\*

\* CNS Department, ENAC

7 av. E. Belin 31055 Toulouse France,

morlaas@enac.fr, chabory@enac.fr, souny@enac.fr.

**Abstract**—Windturbines near VOR ground station can yield significant bearing errors in the azimuth estimation. We propose a model that combines the parabolic equation and the physical optics approximation to predict these errors. It accounts for a possible hilly terrain, and a generic model of windturbines that includes dielectric blades. All the hypotheses made in the model are carefully justified by means of numerical simulations. In a realistic test case, this model is employed to compute the error caused by a complete windfarm located on a hilly terrain within acceptable computation time.

## I. INTRODUCTION

The implementation of windturbines near radionavigation equipments such as VHF omni range (VOR) ground stations is an important concern for civil aviation. The scattering of the signal by the nearby windturbines yields multipath phenomena for the receiver on-board the aircraft. These multipath yield bearing errors in the azimuth estimation, which may render the service unavailable.

Several approaches have been proposed to model the perturbations of windturbines on radio-frequency services, e.g. TV [1] and radar [2]. All of them assume complete metallic windturbines. In [3], a study led specifically for VOR has shown that this hypothesis is no longer valid in the VHF frequency band. This study, that employs the method of moments, requires a 3D CAD model for the windturbines, containing a metallic mast and three dielectric blades. Furthermore, the incident field coming from the VOR ground station is assumed to be a plane wave. Although this approach computes precisely the windturbine scattering, it suffers from its computational cost, and it neglects the terrain profile and dielectric characteristics. Besides, the bearing error can only be computed for a VOR receiver placed in the far field zone of the windturbine.

In this paper, we propose a new approach that can be splitted in three steps. Firstly, in order to take into account the terrain profile and its characteristics, we model the propagation between the ground station and each windturbine with the parabolic equation [4]. This provides a realistic illumination for each windturbine regardless of the distance between the VOR station and the windturbines. Secondly, we compute the scattering of the windturbines using the physical optics approximation. This is realized using a generic and tunable 3D

geometric model for the windturbines. Thirdly, multipath are associated with the scattered field for estimating the bearing error.

## II. CONFIGURATION

In Fig. 1, we represent an example of configuration. The central frequency of the signal is 110MHz. The terrain altitudes and the soil characteristics are known between the ground station and each windturbine. A windturbine is constituted by three elements: a metallic mast of conical shape, a hub modeled by a metallic rectangular box, and three blades which are assumed to be thin multilayer dielectric slabs with constant thickness. The real inner structure of a blade is complex. As in [3], we perform simplifications to end up with two homogeneous dielectric layers separated by air.

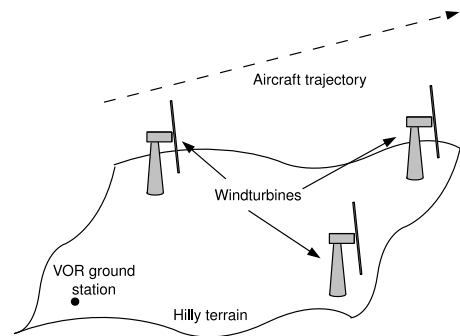


Fig. 1. Example of configuration

## III. PROPAGATION VOR EMITTER / WINDTURBINES

The emitter of the ground station is characterised from the radiation pattern of its antenna. In this article, we use a VOR 431 Thales antenna simulated from Ansoft HFSS, which radiation pattern only depends on the elevation angle. From the ground station to each windturbine, we employ the approach described in [4] in order to compute the forward propagation. This computation is performed step by step at increasing distances, and it accounts for the electrical characteristics of the terrain, a possible ground wave, and the electrical characteristics of the atmosphere. This method is known to be computationally inexpensive and provides realistic incident

fields sampled on the mast axis of each windturbine. Nevertheless, since the backward propagation is neglected, the terrain should not be too steep to obtain accurate results. Furthermore, an azimuthal invariance is assumed, which means that lateral effects are not modeled.

#### IV. SCATTERING OF THE WINDTURBINES

The windturbines are meshed with polygonal facets. Locally on each facet, we assume that the incident field can be approximated by a plane wave. To determine this plane wave for each facet, we start with the result of the parabolic equation, i.e. the incident field sampled on the mast axes. Then, we perform an interpolation to obtain the plane wave propagation axis, polarization, and amplitude.

The mast and the hub are metallic. The currents on their facets are given upon the physical optics approximation. The blades are modeled as dielectric multilayer slabs of constant thickness, therefore, the currents on an illuminated blade facet can be approximated by

$$\begin{aligned} \mathbf{J} &= \mathbf{n} \times (\mathbf{H}_i + \mathbf{H}_r - \mathbf{H}_t), \\ \mathbf{M} &= -\mathbf{n} \times (\mathbf{E}_i + \mathbf{E}_r - \mathbf{E}_t), \end{aligned} \quad (1)$$

in which  $\mathbf{n}$  stands for the facet normal oriented towards the illumination. Furthermore,  $(\mathbf{E}_i, \mathbf{H}_i)$ ,  $(\mathbf{E}_r, \mathbf{H}_r)$ , and  $(\mathbf{E}_t, \mathbf{H}_t)$  represent the incident, reflected and transmitted fields on the facet, respectively. These fields are computed by means of the reflexion/transmission coefficients of the multilayer slab.

Next, we compute the radiation integrals to obtain the field  $\mathbf{E}_n$  scattered by each facet  $n$ . Due to the local plane wave structure of the incident field on each facet, we can employ the Mittra and Lee method described in [5] in order to reduce the computation time of these integrals.

In our approach the mesh size  $D$  must be chosen keeping two criteria in mind. The size  $D$  must be small enough for the local plane wave approximation to hold. Moreover, the Lee and Mittra method is only valid for receivers located in the far-field of each facet. Hence,  $D$  must be small enough so that the distance  $d$  between the receiver and the facets respects the condition  $d < 2D^2/\lambda$ , with  $\lambda$  the wavelength.

Note that the presence of the soil is taken into account in the scattering of windturbines via the theorem of images. Besides, we do not model the multiple scattering between the windturbine elements, e.g. blade-blade, blade-mast or windturbine-windturbine.

#### V. VOR BEARING ERROR

Each facet generates a multipath which relative amplitude and phase are computed by means of the effective height  $\mathbf{h}$  of the receiver antenna. This yields

$$a_n = \left| \frac{\mathbf{E}_n \cdot \mathbf{h}}{\mathbf{E}_i \cdot \mathbf{h}} \right|, \quad \theta_n = \arg\left(\frac{\mathbf{E}_n \cdot \mathbf{h}}{\mathbf{E}_i \cdot \mathbf{h}}\right). \quad (2)$$

In this article, the receiver antenna is supposed to be an ideal isotropic conventional horizontally-polarized antenna.

For VOR, the bearing error induced by the multipath is given by [6]

$$\begin{aligned} \epsilon &= \bar{\varphi} - \varphi \\ &= \arctan \sum_n \frac{a_n \sin(\varphi_n - \varphi) \cos \theta_n}{1 + a_n \sin(\varphi_n - \varphi) \cos \theta_n}, \end{aligned} \quad (3)$$

where  $\varphi$  and  $\bar{\varphi}$  are the actual and estimated azimuth of the receiver with respect to the ground station. Furthermore,  $\varphi_n$  represents the azimuth of the facet  $n$ . A similar expression exists for Doppler VOR [6].

#### VI. NUMERICAL JUSTIFICATIONS OF THE MODEL

##### A. Validation of the blade model

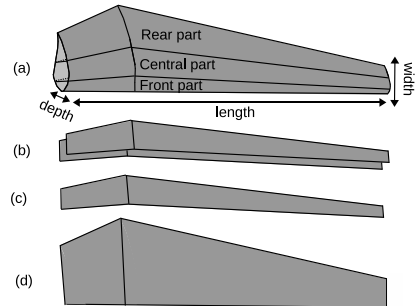


Fig. 2. Different blade models: (a) Full 3D blade, (b) reduced dielectric slab, (c) reduced metallic plate, (d) full metallic plate

To render possible the computation of the windturbine scattering via physical optics, simplifications are employed in the blade structure. In this section, these simplifications are carefully justified by means of simulations with a commercial software, FEKO, which is based on the method of moments (MoM). We start our analysis with a full 3D model as illustrated in Fig. 2(a). The total length of the blade is 37.2 m. Its width and depth vary. Their maximal values are 1.12 m and 0.66 m, respectively. This blade also comprises a lightning protection constituted by a metallic wire. In this model, as numerically validated in [3], the different materials are homogenized to end up with one dielectric layer of relative permittivity  $\epsilon_r = 5$ , and of thickness 4.0, 44.0, and 5.3 mm in the front, central and rear part of the blade, respectively. In order to obtain a multilayer slab of constant thickness, we firstly remove the metallic wire. Secondly, we only keep the central part of the blade because its thickness is significantly larger than the other parts. Thirdly, its depth is approximated as constant. We end up with a reduced dielectric slab. To complete the validation we include two models constituted by metallic plates which size corresponds either to the full blade or its central part.

The configurations of the validations are displayed in Fig. 3. The excitation is provided by a plane wave of frequency 110GHz, with an horizontal polarization and an incidence angle of  $45^\circ$ . We observe at large distance in the horizontal plane. In Fig. 4, we represent the scattered electric field obtained with Feko when the blade is horizontally oriented.

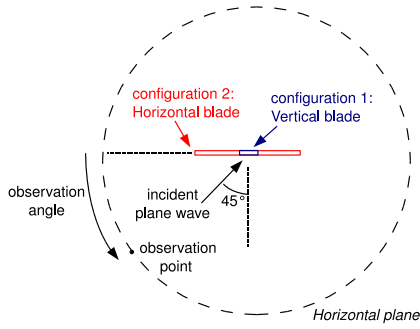


Fig. 3. Configurations used in the validations

We note a good agreement between our blade model and the full 3D model. The levels are well reproduced in all directions of observation. On the other hand, metallic blade models are inefficient since they overestimate strongly the scattered field, even when only the central part of the blade is considered.

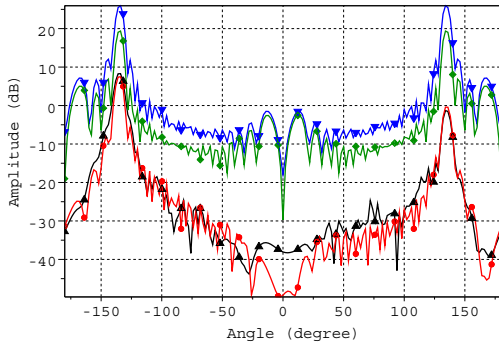


Fig. 4. Normalized scattered electric field by the different blade models for an horizontal blade: full 3D (black with  $\blacktriangle$  markers), reduced dielectric slab (red with  $\bullet$  markers), full metallic plate (blue with  $\blacktriangledown$  markers), reduced metallic plate (green with  $\blacklozenge$  markers).

In Fig. 5, we represent the scattered field when the blade is vertically oriented. This configuration confirms that metallic models overestimate strongly the scattered fields. In the direction of specular transmission, i.e. for observation angles around  $-135^\circ$ , the reduced dielectric slab and the full 3D model fit correctly. In the direction of specular reflexion, i.e. for observation angles around  $+135^\circ$ , differences exist between the two models. The reduced slab yields scattered field few dB greater in this region, which means that the importance of the multipath will be slightly overestimated.

With the model based on a multilayer slab, the blade is simply described by few parameters: the blade sizes (length, width and depth), and the dielectric layer characteristics (thickness and permittivity). This model constitutes a good trade-off between simplicity and accuracy.

### B. Validation of the physical optics approximation

In the previous section, we have validated the model employed for the blade structure. We now numerically check

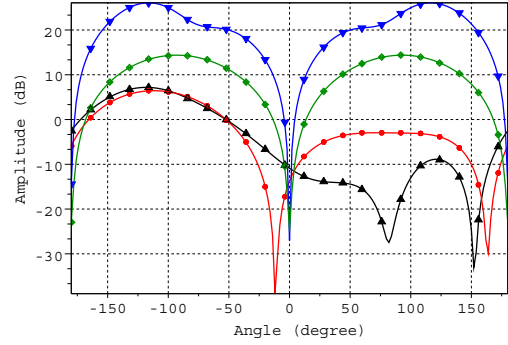


Fig. 5. Normalized scattered electric field by the different blade models for a vertical blade: full 3D (black with  $\blacktriangle$  markers), reduced dielectric slab (red with  $\bullet$  markers), full metallic plate (blue with  $\blacktriangledown$  markers), reduced metallic plate (green with  $\blacklozenge$  markers)

that this model is consistent with the physical optics (PO) approximation. To this end, in the configurations exposed in Fig. 3, we compare the field scattered by the reduced dielectric slab obtained via Feko, and our approach based on the physical optics approximation. The result for an horizontal blade is depicted in Fig. 6. Both approaches match correctly for any observation angle. For the configuration in which the blade is vertical, we observe in Fig. 7 a good agreement near the direction of specular transmission, and slight differences near the direction of specular reflexion. This may be explained by the blade width, which dimension is small enough to reach the limits of the physical optics approximation.

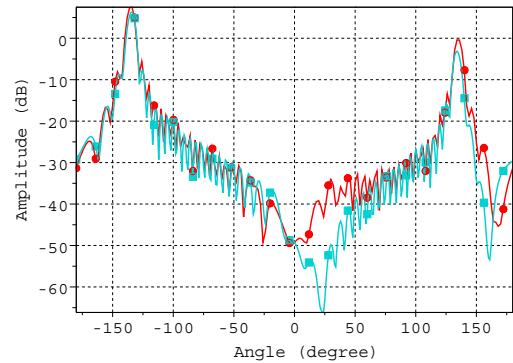


Fig. 6. Normalized scattered electric field by the reduced dielectric slab for a horizontal blade: MoM (red with  $\bullet$  markers), PO (turquoise with  $\blacksquare$  markers)

In the next set of simulations, we compare the field scattered by the mast obtained with Feko and with physical optics. The configuration remains the one of Fig. 3, except for the observation points which are here either in the horizontal or in the vertical plane. In Fig. 8 and Fig. 9, we verify that the physical optics approximation poses no problem to compute the scattering of the mast.

On a multiprocessor computer, the computation time of

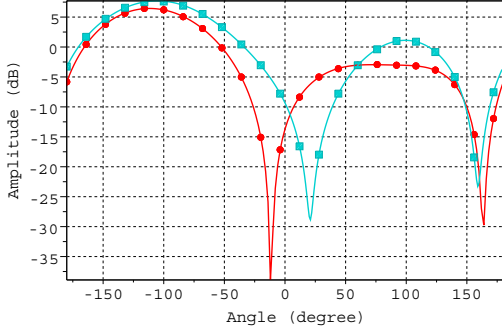


Fig. 7. Normalized scattered electric field by the reduced dielectric blade for a vertical blade: MoM (red with ● markers), PO (turquoise with ■ markers)

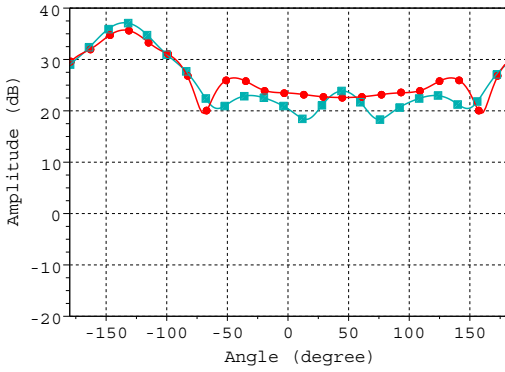


Fig. 8. Normalized scattered electric field by the mast for an observation in the horizontal plane: MoM (red with ● markers), PO (turquoise with ■ markers)

Feko using the parallelized multilevel fast multipole method of moments is about one hour for one blade (reduced dielectric slab) or one mast. On the other hand, with our approach, the scattering of one mast or one blade requires less than one second on a standard desktop computer (one processor). Furthermore, a configuration with several windturbines will yield acceptable computation times because we do not take into account the multiple scattering between windturbine elements. The approach based on physical optics approximation allows to compute the windturbine scattering with a relative good accuracy in acceptable computation times. Hence, this approach is adapted to the estimation of VOR bearing errors.

### C. Justifications of the parabolic equation

In the previous study [3], the windturbine was illuminated by a plane wave. We use here the parabolic equation to compute a realistic incident field on each windturbine. In order to justify this choice, we compute the incident electric field on the vertical axis of a mast obtained with three methods: a plane wave illumination, and the results of the parabolic equation with either a flat or a hilly terrain. The relative permittivity of the ground is of  $\epsilon_r = 25$ . Its conductivity is of  $\sigma = 0.02$ . In

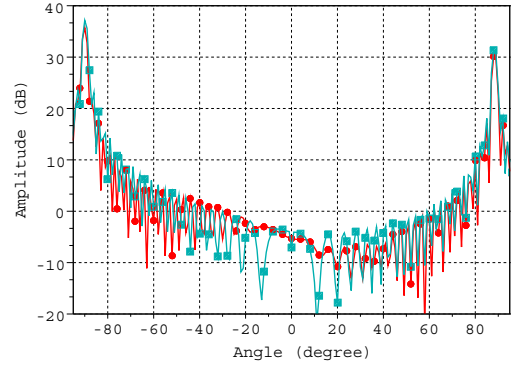


Fig. 9. Normalized scattered electric field by the mast for an observation in the vertical plane: MoM (red with ● markers), PO (turquoise with ■ markers)

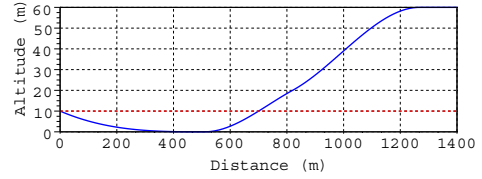


Fig. 10. Altitude profile between the windturbine and the VOR ground station for a flat (red dashed line) or hilly (blue solid line) terrain

Fig. 10, we display the altitude profile. In Fig.11 we compare the incident electric field given by the three methods. We observe significant differences, particularly near the ground level. This result demonstrates the importance of using the parabolic equation to accurately evaluate the incident field on each windturbine. To confirm this result, we show in Fig. 12, the VOR bearing error for an aircraft trajectory at a height of 1067m on the radial of azimuth  $\varphi = 0^\circ$  with respect to the VOR ground station. A windturbine is placed on the radial  $\varphi = 80^\circ$  at 1280m from the ground station. In comparison with the realistic hilly terrain, we observe that the bearing error is significantly overestimated when the illumination is a plane wave, and underestimated when the terrain is assumed flat.

## VII. REALISTIC TEST-CASE

In this section we simulate the realistic scenario described in Fig. 13. The VOR ground station is nearby a windfarm constituted by 21 windturbines. The terrain profile is hilly. The windturbines are placed at distances between 1000m and 2000m from the VOR station. Their blades are all oriented by the wind direction. For each windturbine, the angle of orientation of the 3 blades around the hub axis is randomly chosen from a uniform distribution. Besides, the illumination is obtained via the parabolic equation, with which the terrain profile is accounted.

We compute the VOR bearing error in the vertical plane of azimuth  $\varphi = -10^\circ$ . The result is displayed in Fig. 14. The general threshold level beyond which the VOR service is not

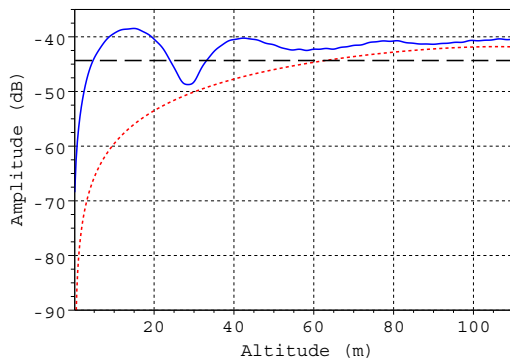


Fig. 11. Incident electric field on the mast axis of the windturbine: plane wave illumination (black dashed line), flat terrain (red dashed line) or hilly terrain (blue solid line) terrain

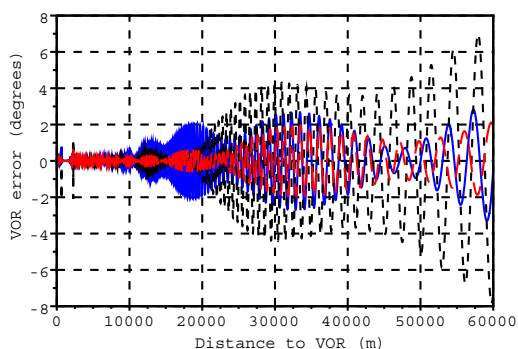


Fig. 12. VOR bearing error (degree): plane wave illumination (black dashed line), flat terrain (red dashed line) or hilly terrain (blue solid line) terrain

considered as available is  $3^\circ$ . Thus we can clearly distinguish in this result the critical area, inside which the VOR error may reach unacceptable values for airplane navigation. In this simulation, the error presents rapid oscillation and can locally have a maximal value of  $55^\circ$ . In an actual receiver, the errors would be smaller because most of the rapid oscillations would be removed by low-pass filtering.

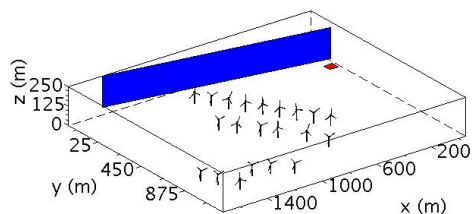


Fig. 13. Configuration of the test-case: windturbines (black), observation plane (blue), VOR ground station (red)

Using a standard desktop computer, the computation at the  $10 \times 100$  observation points has been performed in 7 hours.

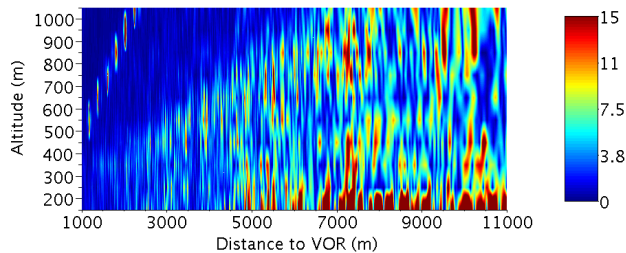


Fig. 14. VOR bearing error (degree) induced by a windfarm of 21 windturbines

Such a scenario was not feasible with the method of moments for two reasons. Firstly the resources of the computer were not sufficient to compute the scattering of 21 windturbines. Secondly, the terrain profile could not be taken into account.

## VIII. CONCLUSION

We have developed a prediction method to model the impact of windturbines onto the azimuth estimation of VOR receivers. This model is based on the parabolic equation and on the physical optics approximation. It accounts for an hilly terrain, and for a generic simplified model of windturbines with dielectric blades.

With numerical tests and comparisons, we have demonstrated the importance of taking account the terrain profile to evaluate the incident field on the windturbines. We have shown that blades approximated by metallic plates lead to a poor efficiency, while a dielectric multilayer structure is fully appropriate. We have also checked that the physical optics approximation is adapted since it realizes a good trade-off between accuracy and computation time.

This tool may be used to determine configurations in which windturbines are troubleless for VOR services.

For future works, a general study could be performed to evaluate separately the relative impact in the bearing error of the masts, the hubs and the blades, so as to determine which element is the most problematic. Parametric and statistical analyses could also be conducted to establish general laws on the co-localization of VOR ground station and windfarm.

## REFERENCES

- [1] BBC/RA/ITC, *The impact of large building and structures (including wind farms) on terrestrial television reception*.
- [2] G. J. Poupart, *Wind farms impact on radar aviation interests - final report*, QinetiQ, Sept. 2003.
- [3] C. Morlaas, M. Fares, B. Souny, "Wind turbine effects on VOR system performance," *IEEE trans. Aerospace and Electronic Systems*, vol. 44, pp. 1464-1476, Feb. 2009.
- [4] G. D. Dockery, J. R. Kuttler, "An improved impedance-boundary algorithm for Fourier Split-Step solutions of the parabolic wave equation," *IEEE trans. Antennas Propag.*, vol. 44, no. 12, Dec. 1996.
- [5] S.W. Lee, R. Mittra, "Fourier transform of a polygonal shape function and its application in electromagnetics," *IEEE trans. Antennas Propag.*, vol. 31, pp. 99-103, Jan. 1983.
- [6] D. Quinet, S. Odunaiya, "Calculations and Analysis of Signal Processing by Various Navigation Receiver Architectures," *Digital Avionics Systems Conference*, vol. 1, Oct. 2004.